Earth and Planetary Science Letters 294 (2010) 101–110

Contents lists available at ScienceDirect

Earth and Planetary Science Letters

journal homepage: www.elsevier.com/locate/epsl

The dependence of chemical weathering rates on fluid residence time

K. Maher

Department of Geological and Environmental Sciences, Braun Hall #118, 450 Serra Mall, Stanford University, Stanford, CA, 94305, USA

ARTICLE INFO

Article history:
Received 13 August 2009
Received in revised form 5 March 2010
Accepted 7 March 2010
Available online 9 April 2010

Editor: M.L. Delaney

Keywords:
weathering
dissolution kinetics
transport-limited
erosion
climate change
feedback

ABSTRACT

In order to evaluate the importance of hydrologic processes in controlling chemical weathering rates, a reactive transport analysis is used to interpret chemical weathering rate data for a range of systems. An analysis of weathering rates for granitic material shows that weathering rates depend most strongly on fluid residence times and fluid flow rates, and depend very weakly on material age. Over moderate fluid residence times from 5 days to 10 yr, characteristic of soils and some aquifers, transport-controlled weathering explains the orders of magnitude variation in weathering rates to a better extent than material age. For fluid residence times greater than 10 yr, characteristic of some aquifers, saprolites, and most marine sediments, a purely thermodynamic-control on chemical weathering rates sustains chemical weathering—this control may be due to clay precipitation, which can drive weathering of primary minerals, or microbial processes which alter the fluid chemistry via the oxidation of organic matter. In addition, this analysis suggests that the apparent time dependence of chemical weathering rates commonly used to model the evolution of Earth's landforms may be attributable to transport-controlled weathering and the evolution of hydrologic properties over time. If hydrologic processes are the primary control on chemical weathering rates, the nature of the temperature dependence of chemical weathering rates is also altered.

1. Introduction

The slow progress towards chemical equilibrium is primarily responsible for the long-term habitability of Earth. Slow kinetics of silicate mineral dissolution enables the development of soils and the growth of both vascular plants and vital microorganisms. Slow dissolution of minerals on land and formation of biogenic calcite in the oceans also maintains atmospheric CO_2 concentrations and therefore plays an important role in maintaining global temperatures at levels optimal for the presence of liquid water (Berner, 1992). In Earth's past, major changes in rock weathering have coincided with periods of mass extinction (Algeo and Scheckler, 1998; Sheldon, 2006) and reorganization of global biogeochemical cycles (Raymo, 1994; Vance et al., 2009).

Although the driving forces behind Earth's weathering engine have been studied extensively for a number of decades, there are at least a few observations of large scale chemical weathering behavior that have not been completely explained, largely because of limited data sets. One behavior of chemical weathering rates that has been particularly enigmatic is the inverse dependence of chemical weathering rates on time (Bain et al., 1993; Taylor and Blum, 1995; White and Brantley, 2003; Maher et al., 2004; Fantle and DePaolo, 2006). A second behavior has been the strong correlation between chemical weathering rates and physical erosion, rates and a weaker correlation between climate and chemical weathering rates (Riebe et al., 2001a; Jacobson et al., 2003; West et al., 2005; Hren et al., 2007).

Hydrology is also potentially an important factor in chemical weathering rates as the removal of weathering products by aqueous transport can drive departure from thermodynamic equilibrium (e.g. transport-controlled weathering). In addition, preferential flow paths may reduce the mineral surface area available to react, or result in a range of chemical conditions along the flow path (Velbel, 1993; Malmstrom et al., 2000; Ganor et al., 2005). In general, chemical weathering rates are expected to accelerate in tandem with flow rates up to a particular threshold where aqueous transport, and by extension the proximity to equilibrium, are no longer limiting and rates are surface reaction-controlled (Berner, 1978; Lasaga et al., 1994; Steefel and Maher, 2009). The distinction between transport-controlled and surface reaction-controlled weathering was perhaps first shown mathematically by Berner (1978) who approximated the weathering system as a well-mixed batch reactor. Observations of etch-pit development in minerals and high degrees of chemical disequilibrium in rivers relative to the rocks they drain have been interpreted as evidence that feldspar weathering rates in natural systems are often surface reaction-controlled, or far enough from equilibrium that intrinsic effects at mineral surfaces control silicate weathering (e.g. Table 1 Berner, 1978; Velbel, 1989). A number of studies have thus investigated the kinetics of aluminosilicate dissolution under a range of far-from-equilibrium conditions. However, the importance of transport-controlled weathering as an underlying factor in the general behavior and apparent time dependence of chemical weathering rates not been thoroughly tested

E-mail address: kmaher@stanford.edu.

0012-821X/$ – see front matter © 2010 Elsevier B.V. All rights reserved.
doi:10.1016/j.epsl.2010.03.010

Table 1
Theoretical equilibration length scales for feldspar minerals calculated using the reactive transport code CrunchFlow under saturated flow conditions.

Flow rate (m/yr)	Equilibration length scales (L_{eq}) at 13 °C					
	K-feldspar (m)		Albite (m)		Anorthite (m)	
0.01	0.9	±0.4	1.6	±0.4	0.9	±0.5
0.1	2.0	±0.7	3.2	±1.0	2.1	±0.6
1.0	15.5	±2.8	27.4	±8.5	17.5	±5.5
10.0	160	±34.4	321.1	±21.4	174	

using soil data from a range of different climates and flow regimes, although a number of studies have now demonstrated the importance of close-to-equilibrium weathering in natural systems (Maher et al., 2006b; Kampman et al., 2009; Maher et al., 2009; White et al., 2009).

1.1. Transport-controlled weathering

Many weathering systems show gradients in solutes and mineral abundances over different characteristic length scales as fluids equilibrate with the solids, characteristic of transport-controlled weathering (Brimhall and Dietrich, 1987; Taylor and Blum, 1995; White et al., 1996; Anderson et al., 2002; Riebe et al., 2003; Nezat et al., 2004; Green et al., 2006; Yoo et al., 2007; Brantley et al., 2008; White et al., 2008; Yoo and Mudd, 2008; Maher et al., 2009; White et al., 2009). In the presence of solute gradients, the well-mixed flow-through reactor approximation has limited interpretive power. Solute gradients are better approximated as flow-through systems, where equilibration of the fluids along a flow path results in a moving reaction front as illustrated by the soil profile model of Fig. 1.

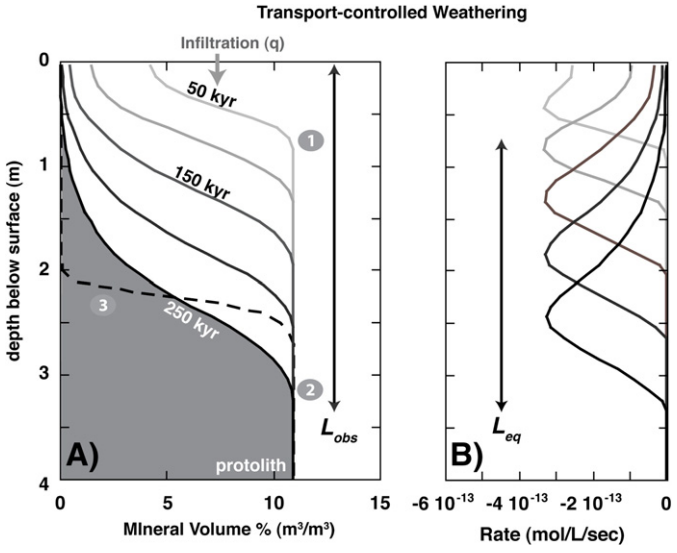

Fig. 1. A) Schematic of transport-controlled weathering showing the evolution of feldspar abundance over time and as a function of depth. B) The corresponding bulk reaction rates [mol/L(porous media)/s] as a function of depth for the profiles in (A). Rates and rate laws used in simulation are experimentally determined laboratory values. L_{obs} corresponds to the observed weathering length scale at the time of measurement (250 kyr). L_{eq} corresponds to the distance over which the fluid equilibrates with the solid and reflects the zone where weathering is occurring. Points on the profiles correspond to key features of transport-controlled weathering. (1) Non-steady-state profile evolution where mineral abundance at the top of the profile has not yet been depleted; (2) steady-state profile evolution where mineral at the top of profile has been mostly depleted and the rate of profile advance becomes constant; (3) an order of magnitude increase in the mineral surface area or kinetic rate constant sharpens the profile but does not appreciably change the mass of material removed due to weathering. The equilibration length scale would also shorten.

The change in overall reaction rate for a given mineral (R_d) as a function of the linear approach to equilibrium occurring along a flow path is commonly defined as (Lasaga, 1984):

$$R_d = -kA\left(1-Q/K_{eq}\right) = -kA(1-\exp(-\Delta G_r/RT)) \quad (1)$$

where A is the mineral surface area (m^2/m^3), k is the kinetic rate constant (mol/m^2/s), and $(1-Q/K_{eq})$ describes the departure from equilibrium, and Q/K_{eq} is the saturation state of the mineral with respect to the fluid. An alternative formulation is provided that makes clear the dependence on reaction affinity (ΔG_r) and temperature (T). Over time, the measured and modeled solute in Fig. 1 reaches equilibrium with the reacting mineral at increasingly greater depths in the soil (L_{obs}), while the overall reaction rate, and thus the distance over which the fluid equilibrates with the solid (L_{eq}), do not change appreciably with time. Clearly, if the solute concentration is measured at a distance greater than L_{eq}, the weathering flux or chemical denudation will be proportional to the flow rate (q) by the equilibrium concentration. Importantly, increases in the intrinsic rate constant and/or mineral surface area will sharpen the profile as L_{eq} decreases, but will not appreciably change the total amount of mass removed (e.g. chemical denudation). Thus, intrinsic mineral kinetics and mineral surface area are only important over relatively short time and length scales and become irrelevant once the system has reached the "local equilibrium limit", or the limit in which the rate constant approaches infinity and the chemical affinity approaches zero (Lichtner, 1993). This condition was originally considered numerically by Lichtner (1993) and was recently validated using a well-studied natural system (Maher et al., 2009). The study by Maher et al. (2009) additionally demonstrated that the rates of secondary mineral precipitation and soil PCO_2 strongly influence the dissolution rate by partly controlling the departure from equilibrium, and that contemporary and long-term weathering rates were equivalent for that site.

The relationship between flow rates and chemical weathering rates has also been explored in a number of studies and variable liquid saturation and preferential flow are the most commonly cited reasons for variability in natural rates due to hydrologic processes (Velbel, 1993; Clow and Drever, 1996; Blum et al., 1998; Malmstrom et al., 2004; Ganor et al., 2005; Hilley and Porder, 2009). However the relationship between flow rates (q) and the departure from equilibrium (ΔG_r) has not been well studied because most natural systems cannot be characterized in sufficient detail. If natural systems are transport-controlled, the bulk reaction rate measured using mass depletion, solute profiles or isotopic approaches should be roughly proportional to the flow rate. The following discussion combines data from natural systems with theoretical considerations to explore evidence for the transport-control of natural systems, and the implications of transport-control for the time dependence of chemical weathering rates and for the role of climate (temperature and rainfall) and tectonics in moderating chemical weathering rates.

2. Materials and methods

2.1. Weathering rates, length scales and fluid residence times in non-eroding environments

Data for chemical weathering rates for granitic alluvial materials were assembled from previous published compilations (White and Brantley, 2003; Maher et al., 2004) or directly from the source articles. No catchment-based data is considered due to the complicated nature of inferring fluid residence times. Because not all studies reported the same physical data, to maintain uniform units (g/g/yr^{-1}) all weathering rate values were converted to original bulk weathering rate units of Maher et al. (2004) using measured surface areas and known formula weights. The relationship between the time constant for weathering R_b (g/g/yr^{-1})

and the Eq. (1) model units of R_d [mol/L_{bulk}/yr] is: R_b[g/g/yr^{-1}]≈ 1−2R_d [mol/L_{bulk}/yr]. Both surface normalized rates and bulk rates were checked against each parameterization and no change in behavior was observed. All data were fit using the curve fit package of Kaliedagraph™.

Fig. 2A shows the decrease in weathering rates as a function of fluid residence time. Fluid residences times (τ_f) are calculated as L_{obs}/v_f (where L_{obs} is the length scale of observation and v_f as the advective velocity). The reported value for L_{obs} reflects the depth to the base of the weathering zone where the mineral abundances in the profile nominally equal the concentration of the soil protolith (cf. Fig. 1) or, for solute flux measurements such as groundwater systems and soils, either groundwater ages or the measurement distance divided by advective flow rate. In order to convert between the percolation flux (q) and the advective velocity, the porosity or volumetric water contents (θ) (unsaturated flow) were used. The uncertainty in converting between flow rates and velocities is not likely to be greater than 20% given the range of porosities and water contents typical of soil systems. A plot of measured fluid flux versus weathering rates suggests that no substantial bias was introduced in the conversion from percolation flux to advective velocity. The data were fit using an exponential function that assumes experimental data represent far-from-equilibrium rates and that the increase in fluid residence time (or decrease in flow rate) reflects the approach to chemical equilibrium (e.g. $(1-\exp(-\Delta G_r/RT))$ in Eq. (1)).

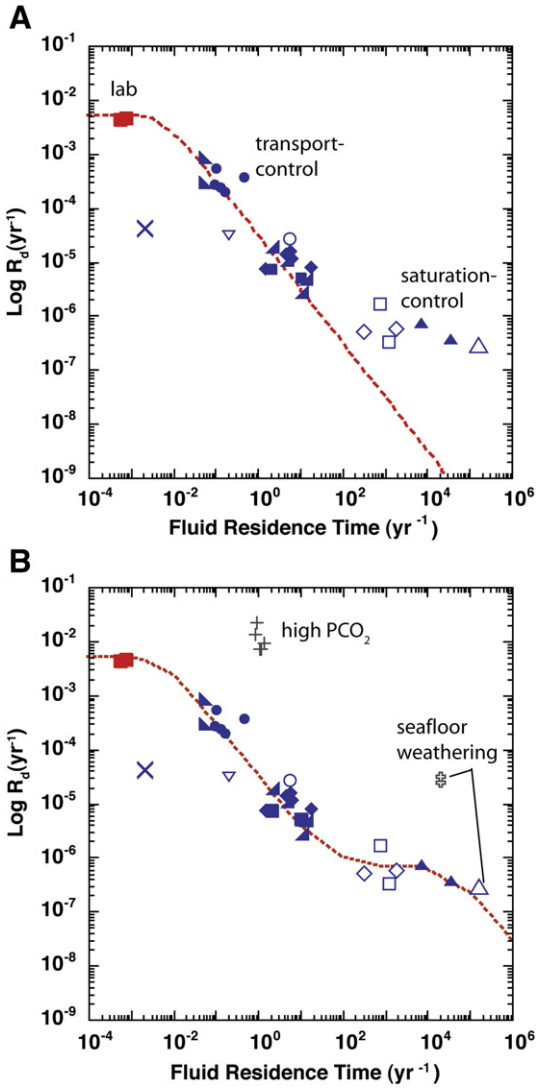

Fig. 2. Bulk weathering rates for feldspar (mostly albite) as a function of fluid residence time in soils. (A) Data from soil and groundwater only - - - - $R_b = 10^{-2.3}(1-\exp(-0.006\times\tau_f^{-1}))$, $R^2=0.98$; ■ Burch et al. (1993); ● Clow and Drever (1996); ▽ Jin et al., (2008); ○ Kenoyer and Bowser (1992); ■ Kim (2002); ◇ Maher et al. (2004); △ Maher et al (2006a); ◣ Swoboda-Colberg and Drever (1993); × White and Brantley (2003); □ White et al. (2001); ◢ White et al. (2005); ◆ White et al. (2008). (B) Fit to extreme weathering systems using composite rate law (see Eq. (7)) and including additional outlying data from: + Navarre-Sitchler and Thyne (2007); ✚ Wallmann et al. (2008).

2.2. Reactive transport approach for equilibration length scales and 1-D erosion

The reactive transport code CrunchFlow (Steefel and Lasaga, 1994; Maher et al., 2006b; Maher et al., 2009) was used to estimate the mineral equilibration length scales (L_{eq}). The model simulations were run at 13 °C and 1 atm. The model domain consisted of a one dimensional soil column with a flux boundary condition at the base of the profile, and a Dirichlet boundary condition for aqueous species at the land–atmosphere interface. The simulations infiltrated dilute rainwater at pH 5.13 into a water-saturated column of minerals with a porosity of 0.25. Rate constants, surface areas and mineral solubilities for albite, K-feldspar and kaolinite and the relevant aqueous complexes are from Maher et al. (2009), while the equilibrium constant value for anorthite is from Arnorsson and Stefansson (1999). The rate constant and surface area for kaolinite will impact the equilibration length because the removal of primary mineral dissolution products by secondary minerals influences the departure from equilibrium (Maher et al., 2009). As a value representative of a natural system, the kaolinite rate constant value determined by Maher et al. (2009) for kaolinite at the Santa Cruz, CA site was used ($10^{-19.20}$mol/m^2/s, 10 m^2/g). The equilibration length scales were calculated once the profiles had reached a steady-state geometric evolution. The equilibration lengths are not sensitive to the initial amount of mineral present, but do vary as a function of the solubilities of other minerals present and the assumed rate constant. For example, the experimental dissolution rate constants for albite and K-feldspar are nominally the same, while the two solubilities are quite different. The result is that K-feldspar equilibration length scale is shorter than for albite or anorthite. In order to address this, one set of simulations was conducted for a monomineralic profile and a second set of simulations with a starting composition approximating granodiorite (64 wt.% plagioclase, 23 wt.% K-feldspar and 13 wt.% quartz) was used to assess the uncertainty on the equilibration length scale as a result of more realistic bulk compositions. Values are summarized in Table 1.

To calculate the L_{eq} values without assuming a large number of arbitrary parameters (soil PCO_2, liquid saturation, etc.) also introduces uncertainty. The assumption of a liquid saturated profile affects the calculated length scales because under field-weathering conditions soil water pH would be strongly impacted by the soil PCO_2. However, under saturated flow conditions the only source of acidity in the model is the rainwater equilibrated with atmospheric CO_2 resulting in a shorter L_{eq}. Surface and areas and rate constants will also change L_{eq}, but will not have an impact on the rate of profile advance.

The reactive transport simulation of erosion using CrunchFlow is adapted directly from the model developed by Maher et al. (2009) for the case of no erosion at the Santa Cruz, CA marine chronosequence. As in the previous study, dilute rainwater is allowed to infiltrate a column of minerals at a known flow rate (0.088 m/yr) and soil PCO_2 is fixed at 0.01 bar. The mineral dissolution rates and precipitation rates are as determined by Maher et al. (2009). To simulate erosion, material is removed at the surface of the fixed reference frame at the specified erosion rate which was assumed to be equal to the weathering advance rate at the site (22.3 mm/kyr). The model was run forward until the profile reached steady state (the mineral profiles remained stationary over time).

3. Results and discussion

3.1. Interpretive model for transport-limited weathering

Assuming that the change in concentration with time at a given location is minimal relative to the change in concentration along the flow path (quasi-steady state), the change in the concentration of an aqueous component (c, [mol/L]) along a flow path (z) as a function of the bulk weathering rate (R_d, [mol/L(bulk porous media)/yr]), porosity (ϕ) and flow rate, (q, [m/yr]), can be written as:

$$\phi\frac{dc}{dt} = 0 = -q\frac{dc}{dz} + R_d\left(1-\frac{c}{c_{eq}}\right) \quad (2)$$

where porosity can be replaced with the volumetric water content for unsaturated zone flow. R_d in this simple case of a one-component system is expanded to account for the moderating effect of chemical equilibrium where c_{eq} is the equilibrium concentration or solubility [mol/L]. The product of these terms is what is commonly calculated for field systems. If Eq. (2) is rearranged, dc/dz is proportional to the balance between the dissolution rate and the flow rate (Johnson and DePaolo, 1997; Maher et al., 2003; Maher et al., 2006a; White et al., 2009) and is moderated by the approach to chemical equilibrium:

$$\frac{dc}{dz} = \frac{R_d}{q}\left(1-\frac{c}{c_{eq}}\right). \quad (3)$$

If we assume that the solute concentration gradient is approximately linear, then the differential term can be approximated as $dc/dz = (c_{eq}-c_o)/L_{eq}$, where L_{eq} is equivalent to the equilibration length scale (cf. Fig. 1) and c_o is the initial concentration. The parameter of $\phi L_{eq}/q$ is representative of the fluid residence time (τ_f). Incorporating these substitutions and assuming that c_o is nominally zero, at distances shorter than L_{eq} the field measured rate is proportional to the product of the flow rate and the concentration:

$$R_d\left(1-c/c_{eq}\right) = q\frac{c_{eq}}{L_{eq}} = \frac{\phi c_{eq}}{\tau_f}. \quad (4)$$

This formulation differs from the original statement of transport-controlled weathering derived by Berner (1978) primarily in terms of the expressed dependence on the length scale. Importantly, at distances greater than L_{eq}, where $c = c_{eq}$, weathering rates are by definition zero and chemical denudation or flux ($c_{eq}q$) conveys no information on the actual weathering kinetics or available surface area. At distances less than the equilibration length scale, actual rates may vary between the full surface reaction-control and transport-control, depending on the distance along the flow path. The equilibration length scale is an important parameter because it apparently controls the rate at which a weathering front advances for a given rate constant and surface area: long equilibration length scales result in faster weathering advance rates and greater mass loss from the profile (Navarre-Sitchler and Brantley, 2007). Thus, in conjunction with biotic and physical disaggregation, the equilibration length scale determines the thickness of soils in a landscape. Equilibrium length scales for major rock forming minerals as a function of flow rate are provided in Table 1. These distances, which are on the order of several meters at typical flow rates, suggest that the approach to equilibrium is likely to be important in most water–rock systems encountered at the Earth's surface.

3.2. Evidence for transport-control of natural systems

While the importance of transport-control is generally recognized, the implications have not been explored in light of weathering rates across a broad range of environments. According to Eq. (4), transport-controlled weathering should result in a relationship between advective transport (τ_f) and the characteristic time for reaction rates ($\phi C_{eq}/R_d$). This relationship is likely to be exponential according to the rate law of Eq. (1). The relative importance of these factors can be evaluated using a common dimensionless parameter, the Damköhler number (Da) (Johnson and DePaolo, 1994; Steefel and Maher, 2009):

$$Da = \frac{\tau_f R_d}{\phi C_{eq}}. \quad (5)$$

For large Damköhler numbers ($Da>1$), reaction is more important than advection and thus the local equilibrium effect is important. Fig. 2A,B shows a strong dependence of bulk weathering rates on fluid residence time, suggesting that many rates for natural systems incorporate the effects of the approach to equilibrium. If laboratory values represent surface reaction-control, then almost all field weathering appears to be transport-controlled. In addition, the data suggest that most natural systems have approximately the same Da number due to overarching thermodynamic effects.

In general, rates should decrease exponentially as a function of ΔG_r. If the departure from equilibrium term of Eq. (1) is the dominant term impacting natural weathering due to gradual equilibration along a flow path, then the decrease in weathering rates can be described in terms of a rate law that depends on fluid residence time rather than purely ΔG_r. An exponential formulation similar to that of Eq. (1) is thus used because it allows rates to reach a plateau where rates no longer depend on transport and are equivalent to the laboratory rate constant of $10^{-2.3}\,yr^{-1}$:

$$R_b\left(yr^{-1}\right) = 10^{-2.3}\left[1-\exp\left(\frac{-0.006\pm0.001}{\tau_f}\right)\right]. \quad (6)$$

This rate law would apply only in systems where the flow rate is constant, and would have to be altered to apply at the catchment scale to account for the distribution of fluid residence times. This model provides some advantages over the empirical fits to the age dependence of weathering rates as it incorporates a modest mechanistic interpretation of the variability in natural weathering rates arising from the effect of transport on chemical equilibrium. The mechanism is the link between the removal of weathering products by flushing and the decline in the overall rate as a system approaches equilibrium. It also provides clear evidence for transport-control of natural weathering rates.

3.3. Weathering in extreme environments

Other mechanisms remove weathering products aside from aqueous transport, thus at long fluid residence times other driving forces for mineral weathering may exist. The change in dissolution behavior from transport-control to a distinct zone of thermodynamic-control is apparent for systems with long fluid residence times (Fig. 2B). Systems with surprising degrees of chemical weathering include deep-sea sediments (Maher et al., 2004, 2006b; Wallmann et al., 2008), saprolites (White et al., 2001; Price et al., 2005) and aquifers (Zhu, 2005). The alternative driving forces in these systems, which may be partly to entirely dominated by diffusive transport, are: 1) the precipitation of secondary minerals (Maher et al., 2006b; Maher et al., 2009; White et al., 2009); and 2) the capacity of microbial activity to sustain departures from equilibrium via reaction networks (Aloisi et al., 2004; Maher et al., 2006b; Wallmann et al., 2008). The potential to drive weathering processes by clay mineral precipitation depends on both the kinetics of clay mineral precipitation relative to the rate of feldspar dissolution (Maher et al., 2006b; Zhu and Lu, 2009), and the role of more soluble pre-cursor minerals (Steefel and

Van Cappellen, 1990). Both processes are challenging to quantify in a natural system. Also, microbial processes that occur in early diagenetic settings produce CO_2 that can be consumed by calcite precipitation and silicate weathering (Maher et al., 2006b; Wallmann et al., 2008; Wu et al., 2008). The effectiveness of this weathering process appears to depend on the organic matter flux to the sediment, which accounts for the difference between weathering rates in deep-sea sediments from Maher et al. (2006a,b) and rates in continental margin sediments from Wallmann et al. (2008). CO_2 consumption by weathering processes along continental margins may rival global continental silicate weathering as a sink for CO_2 (Wallmann et al., 2008). Also shown in Fig. 3B are plagioclase weathering rates calculated from waters draining an active hydrothermal field characterized by high magmatic CO_2 fluxes (Navarre-Sitchler and Thyne, 2007). These data points lie off the general trend of the data but are close to the laboratory values, suggesting surface reaction-control. The difference between this study and other field data may be due to either a strong catalytic effect of CO_2 or uncertainty in surface area determinations.

Despite some variability and the relatively few data points, a pronounced break in the slope of the data in Fig. 3B is apparent. The change in slope most likely defines a region where thermodynamic-control due to either secondary mineral precipitation or microbial processes becomes the dominant driving force for mineral dissolution. A second rate law is assigned to this region, although the rates in sedimentary columns may depend more strongly on organic carbon fluxes than on fluid residence times. If this rate law is combined with the fit to the soils data, a composite rate law can be created:

$$R_b\left(\mathrm{yr}^{-1}\right) = 10^{-2.3}\left[1-\exp\left(\frac{-0.006\pm 0.001}{\tau_f}\right)\right] + 10^{-6.2}\left[1-\exp\left(\frac{-46,300}{\tau_f}\right)\right]. \quad (7)$$

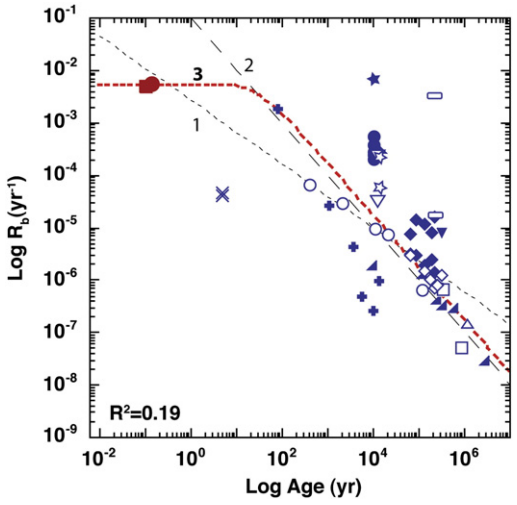

Fig. 3. Bulk weathering rates (R_b) plotted as a function of material or surface age showing the apparent time dependence of bulk chemical weathering rates. Previous suggested fits to the trend along with a new fit (bold stippled line) are also shown. Outliers in the data are from perturbed systems, such as acid rain environments (Kirkwood and Nesbitt, 1991) or systems with extremely high rainfall (Bain et al., 1993). Fits to data: Line 1 is from White and Brantley (2003), $R^2=0.51$; line 2 is from Maher et al. (2004); line 3 (bold stippled line) is fit to the data assuming weathering rates plateau at experimentally determined far-from-equilibrium values, $R_b=10^{-2.3}(1-\exp(-34.6\pm 17\times \mathrm{Age}^{-1}))$, $R^2=0.19$; *Laboratory values*: ■ Burch et al. (1993); ● Knauss and Wolery (1986); × White and Brantley (2003); *Field values:* ✚ Bain et al. (1993); ● Clow and Drever (1996); ▽ Jin et al., (2008); ★ Kirkwood and Nesbitt (1991); ◇ Maher et al. (2004); △ Maher et al. (2006a); Maher et al. (2009); ☆ Swoboda-Colberg and Drever (1993); ○ Taylor and Blum, (1995); ▼ Velbel (1985); ◢ White et al. (1996); □ White et al. (2001); ◆ White et al. (2008).

The behavior of weathering rates over a range of fluid residence times demonstrates the importance of hydrologic *and* biologic processes in controlling chemical weathering rates.

3.4. Implications for the temperature dependence of chemical weathering rates

Accelerated chemical weathering rates and enhanced removal of atmospheric CO_2 during periods of increased global temperatures is also thought to be an important feedback in the global climate system over million-year timescales (Berner, 1992). However, if a weathering system is controlled by fluid transport, the effect of temperature on weathering rates is due largely to changes in the solubility of minerals. For instance, the difference between rates of albite dissolution at 13 °C and 25 °C is a factor of 3 (using an activation energy of 65 kJ/mol suggested by Palandri and Kharaka (2004)). This change in rate is insignificant due to the local equilibrium effect. The change in albite solubility over the same temperature range is about 20%. This may explain in part why it has been challenging to fit Arrhenius-style relationships to describe chemical weathering rates at the catchment scale (e.g. White and Blum, 1995; Kump et al., 2000; Riebe et al., 2004; von Blanckenburg, 2005). If most weathering systems are transport-limited, global models that use the Arrhenius relationship to correct for temperature may be inadequate because the main temperature effect would occur in response to changes in mineral solubility and not mineral kinetics.

In transport-controlled weathering systems flow rates and solubility by definition will be the dominant control on mass removal. The global average continental runoff is 250 mm/yr corresponding to total rainfall of 740 mm/yr. Assuming the runoff values are broadly reflective of infiltration rates through the soil, the global average L_{eq}'s for weathering of albite and K-feldspar at 13 °C are 7.8 m and 4.8 m respectively (Table 1). In a more tropical climate such as the Rio Icacos, Puerto Rico watershed, with average runoff of 3680 mm/yr and average temperature of 22 °C, the equilibration length scale for albite is on the order of 120 m. Total chemical denudation rates should thus be a minimum of 15 times higher in terrains with greater runoff and higher temperatures. From this simple dimensional analysis, which ignores the effects of the bedrock–soil boundaries and seasonality of precipitation, it is likely that many catchments reflect waters that have variably to mostly equilibrated with the local rocks, consistent with the observation that Si fluxes are correlated with annual rainfall (e.g. White and Blum, 1995) and that concentrations remain constant with increasing discharge within a catchment (Godsey et al., 2009).

3.5. Implications for the time dependence of chemical weathering rates

A number of studies have associated the apparent decrease in chemical weathering rates with increasing material age (White and Brantley, 2003; Maher et al., 2004). This relationship is depicted in Fig. 3, along with the previous power law fits to the data and an exponential model that assumes material age only becomes limiting beyond a certain age as a wide array of laboratory experiments generally result in the same maximum rate. Although there are more data points in this compilation ($n=63$) relative to Fig. 2A, the correlation between material age and weathering rates is considerably weaker ($R^2=0.19$) than the correlation between fluid residence time and weathering rates ($R^2=0.98$). In order to understand the potential relationship between the time dependence of weathering rates and transport-controlled weathering, the role of time must examined.

There have been a number of explanations offered for the time dependence shown in Fig. 3 (e.g. Velbel, 1989;1993; White and Brantley, 2003; Maher et al., 2004). However, no singular extrinsic or intrinsic mechanism or combination of mechanisms seems to provide a satisfactory explanation for the overall behavior of chemical

weathering rates through time. Mineral surface areas are known to play a role in the apparent time dependence (Anbeek, 1993; Brantley et al., 1993; Macinnis and Brantley, 1993; White and Brantley, 1995; Hodson et al., 1998b; Hodson et al., 1998a; White and Brantley, 2003). The bulk weathering rates R_b (yr^{-1}) shown in Figs. 2 and 3 reflect directly measured field rates. Field rates are typically normalized using some parameterization of mineral surface area. Mineral surface areas have been shown to increase with time due to increases in surface roughness (White, 1995). However such changes are commonly small—approximately a factor of 10 to 20 over 1 million years of soil weathering (White and Brantley, 2003). Conversely, the effective reactive surface area may decrease over time due to the development of passivating layers, as dissolution consumes mineral defects and step dislocation sites, or as a function of secondary mineral coatings, although it is unclear to what extent the decrease in reactive surface area is offset by the increase in surface area. In general, if the time dependence of chemical weathering rates still exists when mineral surface area is accounted for, and the known effects of time on mineral surface area are expected to be small relative to the five orders of magnitude variation in rates in Fig. 3, then surface area ageing effects can only be a minor contribution to the observed behavior. In addition, a modeling study of chemical weathering found contemporary rates to be equivalent to long-term rates and that laboratory rates could be used to describe the long-term evolution if the non-linear approach to equilibrium was considered (Maher et al., 2009).

The model presented above (e.g. Eq. (6)) includes a potential dependence on time through the use of observational length scales (L_{obs}) used to calculate fluid residence times. This was necessary because very little data exists for L_{eq} aside from that of Table 1. To remove the effect of "time", weathering rates are plotted as a function of purely the flow rate (q), although this greatly reduces the number of data points. Fig. 4 shows the decrease in chemical weathering rates with decreasing flow rates expected for transport-control. A rate law similar to that of Eq. (6) was fit to the data again assuming that a threshold flow rate exists where transport is no longer limiting.

$$R_b\left(yr^{-1}\right) = 10^{-2.3}[1-\exp(-0.06 \pm 0.008{*}q)] \quad (8)$$

The threshold flow rate above which plagioclase dissolution rates become surface reaction-controlled is approximately 16 m/yr, similar

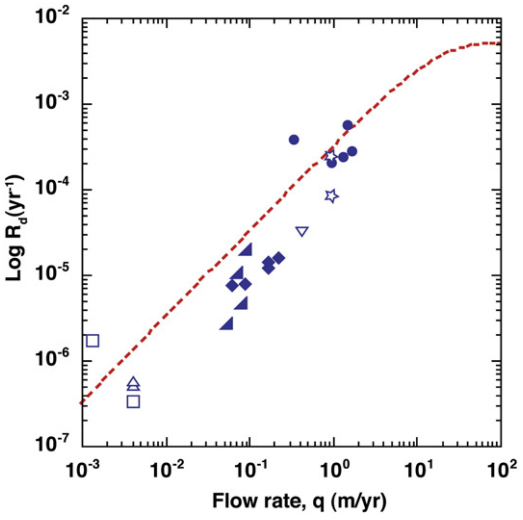

Fig. 4. Correlation between weathering rates and flow rates: - - - - $R_b = 10^{-2.3}(1-\exp(-0.06 \pm 0.008{*}q))$, $R^2 = 0.66$; ● Clow and Drever (1996) ☆ Swoboda-Colberg and Drever (1993); ◢ White et al. (2005); ◆ White et al. (2008); △ Maher et al (2006a); □ White et al. (2001); ▽ Jin et al., (2008).

to the value predicted from Eq. (6). Thus, in order to attribute the time dependence to transport-control, either flow rates/hydraulic properties or rainfall must be correlated with surface age. Shown in Fig. 5A and B is the correlation between flow rate and surface age and rainfall and surface age, respectively. The correlation is best for flow rates, although rainfall may not have been accurately measured at each site as suggested by the clustering of sites. There are a number of explanations for the apparent correlation. First, many chronosequence studies use terraces that vary in elevation. If younger (and higher) terraces receive more rainfall with approximately the same evapotranspiration, then transport-limited weathering would result in the apparent decrease in weathering rates with time. Seasonality may also play a role (Ganor et al., 2005), although this effect is not well investigated in natural systems. Secondly, a sampling bias may also be present because greater fluid fluxes would be required to produce observable weathering on younger surfaces. Thirdly, a decrease in flow rate with time could also result from increasing preferential flow and lower effective hydraulic conductivity as a soil ages and accumulates secondary minerals (Lohse and Dietrich, 2005). Preferential flow would create zones of rapid flow while the matrix fluid may spend longer contact with the grains thus limiting overall dissolution rates. Time dependent changes in flow rate combined with transport-controlled weathering would result in the apparent time dependence of weathering rates, and explain the strong correlation between weathering and material age observed for individual chronosequences. A negative feedback between weathering age and flow rates provides a mechanistic explanation for the apparent time dependence. In contrast, if the correlation is due to a combination of sampling artifacts, then the "age dependence" is entirely an artifact.

3.6. Implications of transport-controlled weathering in active tectonic environments

Accelerated chemical weathering and enhanced removal of atmospheric CO_2 in active tectonic areas has been attributed to the supply of fresh mineral surfaces to the weathering zone through erosion (Stallard and Edmond, 1983; Riebe et al., 2001a; Millot et al., 2002; Jacobson and Blum, 2003; Riebe et al., 2004; von Blanckenburg, 2005; Waldbauer and Chamberlain, 2005; West et al., 2005; Hren et al., 2007). Although long-term CO_2 consumption by silicate weathering due to mountain building may be significantly offset due to substantial carbonate weathering (Jacobson and Blum, 2003), a relationship between chemical fluxes and denudation rates is commonly observed (West et al., 2005; Hren et al., 2007; Gabet and Mudd, 2009). Much of the debate surrounding the capacity of erosion to accelerate chemical weathering rates has focused on the role of mineral supply and mineral surface area while the importance of transport has not been fully evaluated. Under transport-controlled weathering, increasing mineral surface area results in a sharper reaction front, but does not change the equilibrium fluid concentration *or* the rate at which the weathering front propagates downward (Lichtner, 1993; Bolton et al., 2006; Brantley et al., 2008; White et al., 2008; Maher et al., 2009). Given that mountain belts often experience increased rainfall, and that most weathering rates in the absence of erosion appear transport-controlled, the effect of erosion on chemical weathering rates may also be a result of shorter fluid residence times. The prior discussion has focused on stable (non-eroding) alluvial soils primarily because the majority of weathering rate data for natural systems has been collected in these environments. However, the observed decrease is chemical weathering rates with position down slope (Green et al., 2006; Yoo et al., 2007) is generally consistent with transport-control as fluids move downslope.

Many actively eroding environments are composed of an active or mobile soil zone, underlying saprolite and a bedrock interface. A steady-state geomorphic landscape is one where the rate of soil production is equal to the total chemical and physical denudation

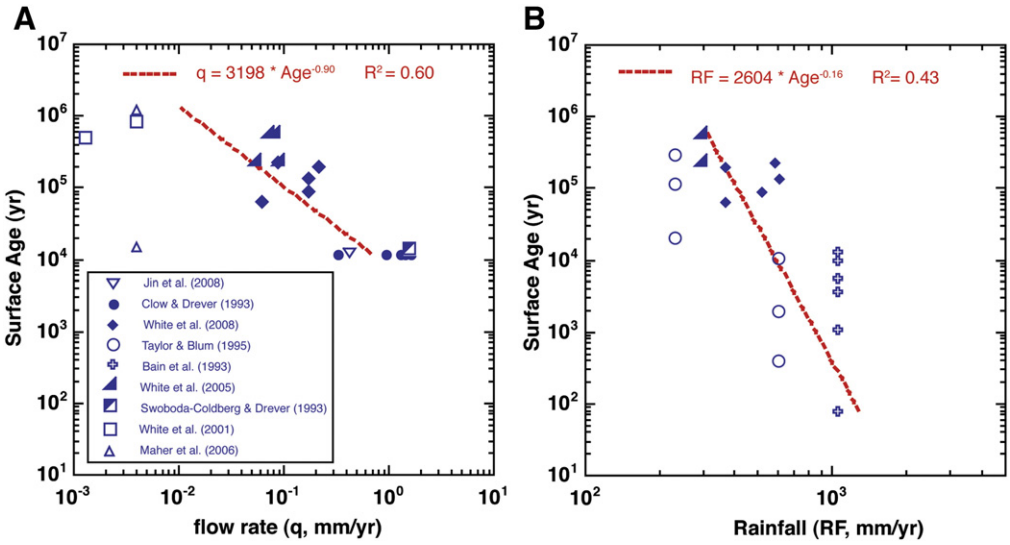

Fig. 5. Correlation between (A) surface age and flow rate (q) and (B) surface age and rainfall (RF), sites shown previously.

rates, resulting in constant soil thickness (L_{obs}) (Heimsath et al., 1997; Riebe et al., 2003). As a simple case, the rate of soil production can be assumed to equal the chemical weathering velocity (ω) depicted in Fig. 1 (Brantley et al., 2008; Buss et al., 2008; White et al., 2008). Biotic and physical factors may also lower the soil–saprolite–bedrock interface at depths greater than the mobile weathering zone, thus in reality the weathering velocity must be less than or equal to the erosion rate in a steady-state landscape. To relate R_d to ω, an expression for the weathering advance rate is required. The change in the volume fraction of mineral, M (m^3/m^3) due to chemical weathering as a function of time and depth is equal to (Lichtner, 1993):

$$\frac{dM}{dt} = \omega \frac{dM}{dz}. \tag{9}$$

The weathering rate controls the change in mass over time. However in the context of a transport-controlled system, the mass removal is controlled by the solute flux and the equilibrium concentration according to Eqs (1) and (2):

$$\frac{dM}{dt} = V_m R_d \left(1 - c/c_{eq}\right) = \frac{qC_{eq}V_m}{L_{eq}} \tag{10}$$

where V_m is the molar volume of the mineral. The change in mineral volume fraction with depth is approximately linear and could be treated similarly to the solute gradient:

$$\frac{dM}{dz} \approx \frac{M_p - M_f}{L_{eq}} \tag{11}$$

where M_p is the volume fraction of mineral in the protolith and M_f is the residual amount in the soil ($M_f \sim 0$). The weathering advance rate can be calculated as:

$$\omega = \frac{qC_{eq}V_m}{M_p - M_f}. \tag{12}$$

This derived expression is similar to that developed and applied by White et al. (2008). Clearly for soil production to equal the weathering velocity requires an extremely finite balance between the hydrology, geochemistry and erosion rate. In general, the residence times of minerals in a soil are much longer than the residence times of fluid in the soil profile (10s of 1000s of years compared to years, respectively). Based on Eq. (7), fluid residence times would have to be less than approximately 2 days (or flow rates on the order of 16 m/yr) for weathering to be surface reaction-controlled and thus dependent purely on the supply of fresh mineral surfaces. Thus, even at high erosion rates equilibration still appears likely. If so, the flux of water should also partly determine weathering rates in eroding terrains due to thermodynamic effects. However, for granitic catchments, no strong correlation between chemical weathering rate and average annual precipitation has been observed, while a correlation between chemical depletion fraction (the mass loss relative to an immobile element) and average annual precipitation has been shown (Riebe et al., 2001b; von Blanckenburg, 2005). The correlation between the chemical weathering rates and denudation rate calculated at the hillslope scale may be due to the effect of erosion on the weathering length scale. Fig. 6 shows a 1-D reactive transport model for steady-state weathering in a stable and eroding soil with no input from upslope (e.g. close to a ridge top). The model confirms that erosion will shorten the equilibration length scale (L_{eq}) and thus the length scale of observed weathering (L_{obs}) relative to a stable soil profile. The

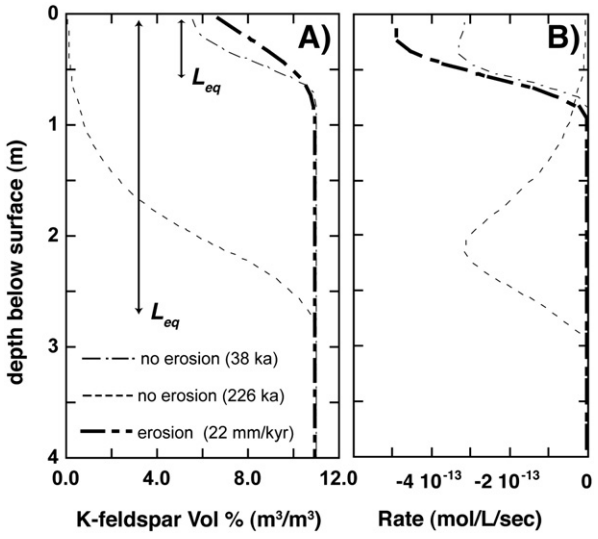

Fig. 6. Reactive transport model (CrunchFlow) simulation of steady-state 1-dimensional erosion for the soil profile from Maher et al. (2009). The light stippled line shows the profiles corresponding to a non-eroding profile under the same conditions ($q = 0.088$ m/yr and the temperature is 12.5 °C). Other minerals included in the simulation are albite, quartz, smectite and kaolinite (not shown) using rates from Maher et al. (2009).

steady-state profile ($\varepsilon = \omega$), would correspond to $L_{eq} = L_{obs} = 0.85$ m and the soil residence time (τ_s) would be approximately 38 ka (Fig. 6). The depth of weathering for a 38 ka non-eroding soil is the same. However, the weathering rate is a factor of two greater for the eroding soil because the overall profile is both farther from equilibrium and surface area is greater, while the chemical flux leaving both the stable and eroding profiles is identical. This suggests that the chemical depletion fraction would be less likely to correlate with denudation rates and more likely to correlate with net infiltration or potentially rainfall, as observed (Riebe et al., 2001a). At the same time, the model confirms that weathering rates should decrease with decreasing erosion rate and increasing soil thickness (Waldbauer and Chamberlain, 2005). Currently there is insufficient data available to test the above hypothesis regarding transport-control in eroding systems, so a simple model is developed to compare the effect of erosion on the weathering length scale to the fluid flux. Because weathering and soil production are inhibited if fluids are at equilibrium, L_{obs} must be less than or equal to the theoretical distance required for the fluid to equilibrate with the solid (L_{eq}). Mathematically this could be stated as $\varepsilon \leq q\ c_{eq} V_m / (M_p - M_f)$. For a given q, as erosion increases and L_{obs} decreases, the weathering rate will increase only once the soil thickness becomes less than the equilibration length scale because the weathering system will be fixed at points farther from thermodynamic equilibrium (e.g. fluid residence time is shorter). Thus Eq. (6), which depends on the fluid residence time should still be operative in an eroding terrain. As the flow rate must be evaluated in conjunction with the erosion rate, the interaction between erosion and climate (via q) on chemical weathering rates can be substituted into Eq. (7) assuming that $L_{eq} = L_{obs} = \varepsilon \tau_s$:

$$R_b\left(\mathrm{yr}^{-1}\right) = 10^{-2.3}\left[1 - \exp\left(-0.006\frac{q}{\tau_s \varepsilon \phi}\right)\right] \quad (13)$$

where R_b is at maximum when $\tau_s \varepsilon\,(L_{obs})$ is $\ll 0.006q$, $10^{-2.3}$ (g/m^2/yr) is the far-from-equilibrium rate constant suggested for non-eroding soils. The potential relationship between soil thickness and weathering rate is shown for different flow rates in Fig. 7. Based on this analysis there are very few soil-mantled regions where granitic weathering is likely surface reaction-controlled and thus dependent purely on mineral surface area (Fig. 7). In general, the model suggests that weathering rates in soils will increase as erosion rates increase and soils thin, and that weathering rates at a given erosion rate will also depend strongly on flow rate. The conceptual formulation may be related to the observation that soil production decreases exponentially with increasing soil thickness (Heimsath et al., 1997), and that chemical denudation rates decrease with increasing soil thickness and position downslope (Burke et al., 2007; Yoo et al., 2007).

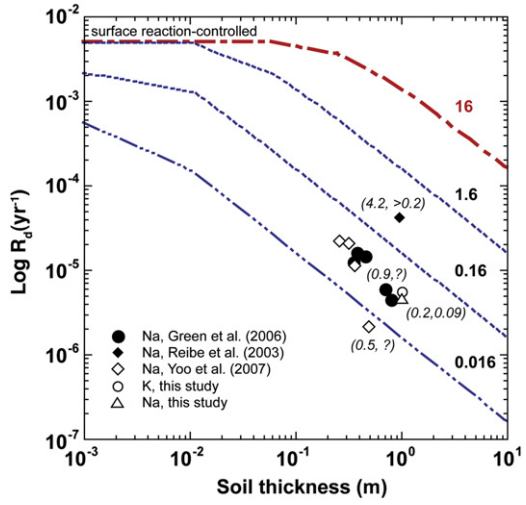

Fig. 7. Interpretive model (e.g. Eq. (13)) for variation in chemical weathering rates in soil profiles from eroding terrains showing the balance between soil residence time and fluid flow rate, assuming upward advection of material through the soil zone and removal at the surface. The bold stippled curve corresponds to the predicted upper envelope of the transport-controlled weathering zone from Eq. (6). Contrary to the case with no erosion, rates decrease as the soil becomes thicker because of the longer equilibration length scale imposed by the assumption that L_{eq} equals L_{obs} for steady-state erosion. The rainfall and the known fluid flow rate are given in parentheses next to the adjacent data points respectively. Model data points from this study are calculated from albite and K-feldspar profiles derived from the reactive transport simulation of Fig. 6.

The implications of this model are that in eroding terrains with appreciable soil development that lie under the envelope of transport-controlled weathering, deciphering the controls on chemical weathering rates at the catchment scale may be challenging because of the critical role that fluid residence time plays in regulating the chemical weathering rate. Fluids that have equilibrated with soil and saprolite minerals reflect chemical fluxes but do not provide a measure of the role of fresh mineral surfaces. Transport-limited weathering would suggest that enhanced chemical fluxes in actively eroding areas are partly due to faster flushing rates and the weak response of mineral solubilities to temperature, implying that other aspects of mountain building, in addition to the production of fresh mineral surfaces through erosion, may drive accelerated chemical weathering.

4. Conclusion

An analysis of the relationship between flow rates, fluid residence times and chemical weathering rates suggests that the time dependence may result from the ubiquity of transport-controlled weathering. Typical hydrologic fluxes at the Earth's surface are slow enough that transport-controlled weathering is likely to characterize the weathering of most granitic sediments. Transport limitation appears to begin as fluid residence times exceed approximately 2 days and flow rates exceed 16 m/yr. While the effects of aqueous transport on chemical weathering rates may not be purely a result of the departure from chemical equilibrium, the effect of transport clearly plays a critical role in moderating chemical weathering rates at the Earth's surface, as hypothesized by previous studies (Berner, 1978; White and Blum, 1995; Kump et al., 2000). At fluid residence times on the order of several hundred years consistent typical of diffusion-dominated environments, a second controlling factor appears to exist. Weathering in this thermodynamically-limited zone may be controlled by other chemical driving forces such as Ostwald ripening and clay precipitation, or by microbial processes and the flux of organic carbon to a site. This region of chemical weathering occupies large fractions of the Earth's surface and is capable of playing a substantial role in moderating the global CO_2 budget, but is not sufficiently well characterized to allow for global-scale predictions.

The predominance of transport-limited weathering implies that 1) chemical weathering rates are more strongly dependent on fluid flow, pH and mineral solubility than mineral surface area and mineral kinetics; 2) the temperature dependence of silicate weathering rates will not be well characterized by Arrhenius-style rate laws, but rather by the temperature dependence of mineral solubilities, which dampens the response of chemical weathering rates to temperature, and 3) erosion will accelerate chemical weathering but this effect will be strongly moderated by the flow rate and other factors that impact the departure from thermodynamic equilibrium.

Acknowledgments

This work was supported by NSF grant EAR-0921134. M. Delaney, A. Jacobsen and an anonymous reviewer are acknowledged for their helpful reviews and constructive comments. S. Moon and C. P. Chamberlain are acknowledged for their thoughtful comments on an earlier version of this manuscript.

References

Algeo, T.J., Scheckler, S.E., 1998. Terrestrial–marine teleconnections in the Devonian: links between the evolution of land plants, weathering processes, and marine anoxic events. Philos. Trans. R. Soc. Lond. Ser. B-Biol. Sci. 353 (1365), 113–128.

Aloisi, G., Wallmann, K., Drews, M., 2004. Evidence for the submarine weathering of silicate minerals in Black Sea sediments: possible implications for the marine Li and B cycles. Geochem. Geophys. Geosyst. 5.

Anbeek, C., 1993. The effect of natural weathering on dissolution rates. Geochim. Cosmochim. Acta 57 (21–22), 4963–4975.

Anderson, S.P., Dietrich, W.E., Brimhall, G.H., 2002. Weathering profiles, mass-balance analysis, and rates of solute loss: linkages between weathering and erosion in a small, steep catchment. Geol. Soc. Amer. Bult. 114 (9), 1143–1158.

Arnorsson, S., Stefansson, A., 1999. Assessment of feldspar solubility constants in water in the range 0 degrees to 350 degrees C at vapor saturation pressures. Am. J. Sci. 299 (3), 173–209.

Bain, D.C., Mellor, A., Robertson-Rintoul, M.S.E., Buclkand, S.T., 1993. Variations in weathering processes and rates with time in a chronosequence of soils from Glen-Feshie, Scotland. Geoderma 57 (3), 275–293.

Berner, R.A., 1978. Rate control of mineral dissolution under earth surface conditions. Am. J. Sci. 278 (9), 1235–1252.

Berner, R.A., 1992. Weathering, plants, and the long-term carbon-cycle. Geochim. Cosmochim. Acta 56 (8), 3225–3231.

Blum, J.D., Gazis, C.A., Jacobson, A.D., Chamberlain, C.P., 1998. Carbonate versus silicate weathering in the Raikhot watershed within the high Himalayan crystalline series. Geology 26 (5), 411–414.

Bolton, E.W., Berner, R.A., Petsch, S.T., 2006. The weathering of sedimentary organic matter as a control on atmospheric O-2: II. Theoretical modeling. Am. J. Sci. 306 (8), 575–615.

Brantley, S.L., Blai, A.C., Cremeens, D.L., Macinnis, I., Darmody, R.G., 1993. Natural etching rates of feldspar and hornblende. Aquat. Sci. 55 (4), 262–272.

Brantley, S.L., Bandstra, J., Moore, J., White, A.F., 2008. Modelling chemical depletion profiles in regolith. Geoderma 145 (3–4), 494–504.

Brimhall, G.H., Dietrich, W.E., 1987. Constitutive mass balance relations between chemical-composition, volume, density, porosity, and strain in metasomatic hydrochemical systems — results on weathering and pedogenesis. Geochim. Cosmochim. Acta 51 (3), 567–587.

Burch, T.E., Nagy, K.L., Lasaga, A.C., 1993. Free-energy dependence of albite dissolution kinetics at 80-degrees-C and Ph 8.8. Chem. Geol. 105 (1–3), 137–162.

Burke, B.C., Heimsath, A.M., White, A.F., 2007. Coupling chemical weathering with soil production across soil-mantled landscapes. Earth Surf. Proc. Landf. 32 (6), 853–873.

Buss, H.L., Sak, P.B., Webb, S.M., Brantley, S.L., 2008. Weathering of the Rio Blanco quartz diorite, Luquillo Mountains, Puerto Rico: coupling oxidation, dissolution, and fracturing. Geochim. Cosmochim. Acta 72 (18), 4488–4507.

Clow, D.W., Drever, J.I., 1996. Weathering rates as a function of flow through an alpine soil. Chem. Geol. 132 (1–4), 131–141.

Fantle, M.S., DePaolo, D.J., 2006. Sr isotopes and pore fluid chemistry in carbonate sediment of the Ontong Java Plateau: calcite recrystallization rates and evidence for a rapid rise in seawater Mg over the last 10 million years. Geochim. Cosmochim. Acta 70 (15), 3883–3904.

Gabet, E.J., Mudd, S.M., 2009. A theoretical model coupling chemical weathering rates with denudation rates. Geology 37 (2), 151–154.

Ganor, J., Roueff, E., Erel, Y., Blum, J.D., 2005. The dissolution kinetics of a granite and its minerals — implications for comparison between laboratory and field dissolution rates. Geochim. Cosmochim. Acta 69 (3), 607–621.

Godsey, S.E., Kirchner, J.W., Clow, D.W., 2009. Concentration–discharge relationships reflect chemostatic characteristics of US catchments. Hydrol. Proc. 23 (13), 1844–1864.

Green, E.G., Dietrich, W.E., Banfield, J.F., 2006. Quantification of chemical weathering rates across an actively eroding hillslope. Earth Planet. Sci. Lett. 242 (1–2), 155–169.

Heimsath, A.M., Dietrich, W.E., Nishiizumi, K., Finkel, R.C., 1997. The soil production function and landscape equilibrium. Nature 388 (6640), 358–361.

Hilley, G.E., Porder, S., 2009. A framework for predicting global silicate weathering and CO_2 drawdown rates over geologic time-scales. Proc. Natl. Acad. Sci. U. S. A. 105 (44), 16855–16859.

Hodson, M.E., Langan, S.J., Meriau, S., 1998a. Determination of mineral surface area in relation to the calculation of weathering rates. Geoderma 83 (1–2), 35–54.

Hodson, M.E., Langan, S.J., Kennedy, F.M., Bain, D.C., 1998b. Variation in soil surface area in a chronosequence of soils from Glen Feshie, Scotland and its implications for mineral weathering rate calculations. Geoderma 85 (1), 1–18.

Hren, M.T., Hilley, G.E., Chamberlain, G.P., 2007. The relationship between tectonic uplift and chemical weathering rates in the Washington cascades: field measurements and model predictions. Am. J. Sci. 307 (9), 1041–1063.

Jacobson, A.D., Blum, J.D., 2003. Relationship between mechanical erosion and atmospheric CO_2 consumption in the New Zealand Southern Alps. Geology 31 (10), 865–868.

Jacobson, A.D., Blum, J.D., Chamberlain, C.P., Craw, D., Koons, P.O., 2003. Climatic and tectonic controls on chemical weathering in the New Zealand Southern Alps. Geochim. Cosmochim. Acta 67 (1), 29–46.

Jin, L.X., Hamilton, S.K., Walter, L.M., 2008. Mineral weathering rates in glacial drift soils (SW Michigan, USA): new constraints from seasonal sampling of waters and gases at soil monoliths. Chemical Geology 249 (1–2), 129–154.

Johnson, T.M., DePaolo, D.J., 1994. Interpretation of isotopic data in groundwater–rock systems — model development and application to Sr isotope data from Yucca Mountain. Water Resour. Res. 30 (5), 1571–1587.

Johnson, T.M., DePaolo, D.J., 1997. Rapid exchange effects on isotope ratios in groundwater systems. 1. Development of a transport-dissolution-exchange model. Water Resour. Res. 33 (1), 187–195.

Kampman, N., Bickle, M., Becker, J., Assayag, N., Chapman, H., 2009. Feldspar dissolution kinetics and Gibbs free energy dependence in a CO_2-enriched groundwater system, Green River, Utah. Earth Planet. Sci. Lett. 284 (3–4), 473–488.

Kenoyer, G.J., Bowser, C.J., 1992. Groundwater chemical evolution in a sandy silicate aquifer in Northern Wisconsin. 2. Reaction modeling. Water Resour. Res. 28 (2), 591–600.

Kim, K., 2002. Plagioclase weathering in the groundwater system of a sandy, silicate aquifer. Hydrol. Proc. 16 (9), 1793–1806.

Kirkwood, D.E., Nesbitt, H.W., 1991. Formation and evolution of soils from an acidified watershed: Plastic Lake, Ontario, Canada. Geochim. Cosmochim. Acta 55 (5), 1295–1308.

Knauss, K.G., Wolery, T.J., 1986. Dependence of albite dissolution kinetics on Ph and time at 25-degrees-C and 70-degrees-C. Geochim. Cosmochim. Acta 50 (11), 2481–2497.

Kump, L.R., Brantley, S.L., Arthur, M.A., 2000. Chemical weathering, atmospheric CO_2, and climate. Annu. Rev. Earth Planet. Sci. 28, 611–667.

Lasaga, A.C., 1984. Chemical-kinetics of water–rock interactions. J. Geophys. Res. 89 (NB6), 4009–4025.

Lasaga, A.C., Soler, J.M., Ganor, J., Burch, T.E., Nagy, K.L., 1994. Chemical-weathering rate laws and global geochemical cycles. Geochim. Cosmochim. Acta 58 (10), 2361–2386.

Lichtner, P.C., 1993. Scaling properites of time–space kinetic mass transport equations and the local equilibrium limit. Am. J. Sci. 293, 257–296.

Lohse, K.A., Dietrich, W.E., 2005. Contrasting effects of soil development on hydrological properties and flow paths. Water Resour. Res. 41 (12).

Macinnis, I.N., Brantley, S.L., 1993. Development of etch pit size distributions on dissolving minerals. Chem. Geol. 105 (1–3), 31–49.

Maher, K., DePaolo, D.J., Conrad, M.E., Serne, R.J., 2003. Vadose zone infiltration rate at Hanford, Washington, inferred from Sr isotope measurements. Water Resour. Res. 39 (8), 1029–1043.

Maher, K., DePaolo, D.J., Lin, J.C.F., 2004. Rates of silicate dissolution in deep-sea sediment: in situ measurement using U-234/U-238 of pore fluids. Geochim. Cosmochim. Acta 68 (22), 4629–4648.

Maher, K., DePaolo, D.J., Christensen, J.N., 2006a. U–Sr isotopic speedometer: flow and chemical weathering in aquifers. Geochim. Cosmochim. Acta 70 (17), 4417–4435.

Maher, K., Steefel, C.I., DePaolo, D.J., Viani, B.E., 2006b. The mineral dissolution rate conundrum: insights from reactive transport modeling of U isotopes and pore fluid chemistry in marine sediments. Geochim. Cosmochim. Acta 70 (2), 337–363.

Maher, K., White, A.F., Steefel, C.I., Stonestrom, D.A., 2009. The role of secondary minerals and reaction affinity in regulating weathering rates at the Santa Cruz marine terrace chronosequence. Geochim. Cosmochim. Acta 73, 2804–2831.

Malmstrom, M.E., Destouni, G., Banwart, S.A., Stromberg, B.H.E., 2000. Resolving the scale-dependence of mineral weathering rates. Environ. Sci. Technol. 34 (7), 1375–1378.

Malmstrom, M.E., Destouni, G., Martinet, P., 2004. Modeling expected solute concentration in randomly heterogeneous flow systems with multicomponent reactions. Environ. Sci. Technol. 38 (9), 2673–2679.

Millot, R., Gaillardet, J., Dupre, B., Allegre, C.-J., 2002. The global control of silicate weathering rates and the coupling with physical erosion; new insights from rivers of the Canadian Shield. Earth Planet. Sci. Lett. 196 (1–2), 83–98.

Navarre-Sitchler, A., Brantley, S., 2007. Basalt weathering across scales. Earth Planet. Sci. Lett. 261 (1–2), 321–334.

Navarre-Sitchler, A., Thyne, G., 2007. Effects of carbon dioxide on mineral weathering rates at earth surface conditions. Chem. Geol. 243 (1–2), 53–63.

Nezat, C.A., Blum, J.D., Klaue, A., Johnson, C.E., Siccama, T.G., 2004. Influence of landscape position and vegetation on long-term weathering rates at the Hubbard Brook Experimental Forest, New Hampshire, USA. Geochim. Cosmochim. Acta 68 (14), 3065–3078.

Palandri, J.L., Kharaka, Y.K., 2004. A compilation of rate parameters of water–mineral interaction kinetics for application to geochemical modeling *Rep. 2004-1068*. US Geological Survey Open File Report.

Price, J.R., Velbel, M.A., Patino, L.C., 2005. Rates and time scales of clay-mineral formation by weathering in saprolitic regoliths of the southern Appalachians from geochemical mass balance. Geol. Soc. Am. Bull. 117 (5–6), 783–794.

Raymo, M.E., 1994. The Himalayas, organic-carbon burial, and climate in the Miocene. Paleoceanography 9 (3), 399–404.

Riebe, C.S., Kirchner, J.W., Granger, D.E., Finkel, R., 2001a. Strong tectonic and weak climatic control of long-term chemical weathering rates. Geol. Soc. Am. Bull. 29 (6), 511–514.

Riebe, C.S., Kirchner, J.W., Granger, D.E., Finkel, R.C., 2001b. Minimal climatic control on erosion rates in the Sierra Nevada. Calif. Geol. 29 (5), 447–450.

Riebe, C.S., Kirchner, J.W., Finkel, R.C., 2003. Long-term rates of chemical weathering and physical erosion from cosmogenic nuclides and geochemical mass balance. Geochim. Cosmochim. Acta 67 (22), 4411–4427.

Riebe, C.S., Kirchner, J.W., Finkel, R., 2004. Erosional and climatic effects on long-term chemical weathering rates in granitic landscapes spanning diverse climate regimes. Earth Planet. Sci. Lett. 224, 547–562.

Sheldon, N.D., 2006. Abrupt chemical weathering increase across the Permian–Triassic boundary. Paleogeogr. Paleoclimatol. Paleoecol. 231 (3–4), 315–321.

Stallard, R.F., Edmond, J.M., 1983. Geochemistry of the Amazon. 2. The influence of geology and weathering environment on the dissolved-load. J. Geophys. Res.-Oceans Atmos. 88 (NC14), 9671–9688.

Steefel, C.I., Lasaga, A.C., 1994. A coupled model for transport of multiple chemical-species and kinetic precipitation dissolution reactions with application to reactive flow in single-phase hydrothermal systems. Am. J. Sci. 294 (5), 529–592.

Steefel, C.I., Maher, K., 2009. Fluid–rock interaction: a reactive transport approach. Reviews in Mineralogy & Geochemistry. Mineralogical Society of America, pp. 485–532.

Steefel, C.I., Van Cappellen, P., 1990. A new kinetic approach to modeling water–rock interaction — the role of nucleation, precursors, and Ostwald ripening. Geochim. Cosmochim. Acta 54 (10), 2657–2677.

Swoboda-Colberg, N.G., Drever, J.I., 1993. Mineral dissolution rates in plot-scale field and laboratory experiments. Chem. Geol. 105 (1–3), 51–69.
Taylor, A., Blum, J.D., 1995. Relation between soil age and silicate weathering rates determined from the chemical evolution of a glacial chronosequence. Geology 23 (11), 979–982.
Vance, D., Teagle, D.A.H., Foster, G.L., 2009. Variable Quaternary chemical weathering fluxes and imbalances in marine geochemical budgets. Nature 458 (7237), 493–496.
Velbel, M.A., 1985. Geochemical mass balances and weathering rates in forested watersheds of the Southern Blue Ridge. Am. J. Sci. 285 (10), 904–930.
Velbel, M.A., 1989. Effect of chemical affinity on feldspar hydrolysis rates in 2 natural weathering systems. Chem. Geol. 78 (3–4), 245–253.
Velbel, M.A., 1993. Constancy of silicate mineral weathering-rate ratios between natural and experimental weathering — implications for hydrologic control of differences in absolute rates. Chem. Geol. 105 (1–3), 89–99.
von Blanckenburg, F., 2005. The control mechanisms of erosion and weathering at basin scale from cosmogenic nuclides in river sediment. Earth Planet. Sci. Lett. 237 (3–4), 462–479.
Waldbauer, J.R., Chamberlain, C.P., 2005. Influence of uplift, weathering and base cation supply on past and future CO_2 levels. A history of atmospheric CO_2 and its effects on plants, animals and ecosystems. In: E., et al. (Ed.), Ecological Studies 177: a History of Atmospheric CO_2 and its Effects on Plants, Animals and Ecosystems, pp. 166–184.
Wallmann, K., Aloisi, G., Tischenko, P., Pavlova, G., Greinert, J., Kutterolf, S., Eisenhauer, A., 2008. Silicate weathering in anoxic marine sediments. Geochim. Cosmochim. Acta 3067–3090.
West, A.J., Galy, A., Bickle, M., 2005. Tectonic and climatic controls on silicate weathering. Earth Planet. Sci. Lett. 235 (1–2), 211–228.
White, A.F., 1995. Chemical weathering rates of silicate minerals is soils. Chemical Weathering Rates of Silicate Minerals. Mineralogical Society of America, pp. 407–461.
White, A.F., Blum, A.E., 1995. Effects of climate on chemical-weathering in watersheds. Geochim. Cosmochim. Acta 59 (9), 1729–1747.
White, A.F., Brantley, S.L., 1995. Chemical weathering rates of silicate minerals: an overview. Chemical Weathering Rates of Silicate Minerals. Mineralogical Society of America, pp. 1–22.
White, A.F., Brantley, S.L., 2003. The effect of time on the weathering of silicate minerals: why do weathering rates differ in the laboratory and field? Chem. Geol. 202 (3–4), 479–506.
White, A.F., Blum, A.E., Schulz, M.S., Bullen, T.D., Harden, J.W., Peterson, M.L., 1996. Chemical weathering rates of a soil chronosequence on granitic alluvium. 1. Quantification of mineralogical and surface area changes and calculation of primary silicate reaction rates. Geochim. Cosmochim. Acta 60 (14), 2533–2550.
White, A.F., Bullen, T.D., Schulz, M.S., Blum, A.E., Huntington, T.G., Peters, N.E., 2001. Differential rates of feldspar weathering in granitic regoliths. Geochim. Cosmochim. Acta 65 (6), 847–869.
White, A.F., Schulz, M.S., Vivit, D.V., Blum, A.E., Stonestrom, D.A., Harden, J.W., 2005. Chemical weathering rates of a soil chronosequence on granitic alluvium: III. Hydrochemical evolution and contemporary solute fluxes and rates. Geochim. Cosmochim. Acta 69 (8), 1975–1996.
White, A.F., Schulz, M.S., Vivit, D.V., Blum, A., Stonestrom, D.A., Anderson, S.P., 2008. Chemical weathering of a marine terrace chronosequence, Santa Cruz, California I: interpreting the long-term controls on chemical weathering based on spatial and temporal element and mineral distributions. Geochim. Cosmochim. Acta 72 (1), 36–68.
White, A.F., Schulz, M.S., Stonestrom, D.A., Vivit, D.V., Fitzpatrick, J., Bullen, T., Maher, K., Blum, A.E., 2009. Chemical weathering of a marine terrace chronosequence, Santa Cruz, California II: controls on solute fluxes and comparisons of long-term and contemporary mineral weathering rates. Geochim. Cosmochim. Acta 73, 2769–2803.
Wu, L.L., Jacobson, A.D., Hausner, M., 2008. Characterization of elemental release during microbe–granite interactions at T=28 degrees C. Geochim. Cosmochim. Acta 72 (4), 1076–1095.
Yoo, K., Mudd, S.M., 2008. Discrepancy between mineral residence time and soil age: implications for the interpretation of chemical weathering rates. Geology 36 (1), 35–38.
Yoo, K., Amundson, R., Heimsath, A.M., Dietrich, W.E., Brimhall, G.H., 2007. Integration of geochemical mass balance with sediment transport to calculate rates of soil chemical weathering and transport on hillslopes. J. Geophys. Res.-Earth Surf. 112 (F2).
Zhu, C., 2005. In situ feldspar dissolution rates in an aquifer. Geochim. Cosmochim. Acta 69 (6), 1435–1453.
Zhu, C., Lu, P., 2009. Alkali feldspar dissolution and secondary mineral precipitation in batch systems: 3. Saturation states of product minerals and reaction paths. Geochim. Cosmochim. Acta 73 (11), 3171–3200.